

# VISCOUS EFFECTS ON THE HYDRODYNAMIC PERFORMANCE OF SEMI-ACTIVE FLAPPING PROPULSOR

NONTHIPAT THAWEEWAT\*, SURASAK PHOEMSAPTHAWEE AND SIRIRAT JUNGRUNGRUENGTAWORN

Department of Maritime Engineering  
Faculty of International Maritime Studies, Kasetsart University  
199 Moo 6, Sukhumvit Rd, Sriracha, Chonburi 20230, Thailand  
\*e-mail: nonthipat.t@ku.th

**Key words:** Flapping foil, Biomimetics, Propulsion

**Abstract.** A numerical tool based on Lattice Boltzmann Method is used to investigate viscous effects on the hydrodynamic performance of a semi-active flapping propulsor. The obtained viscous results are compared with potential flow results previously presented in literature. It is found that both numerical tools give a qualitatively good trend agreement of the open water performance at high equivalent advance numbers. The results obtained using the viscous solver are slightly lower than that of potential flow in the region where flow separation is not observed. However, in case of small equivalent advance numbers, serious flow separation occurs due to high angle of attack, and hence the viscous results yield significantly lower efficiency. In spite of the mentioned deviation in the performance predictions, the LBM results confirm that the semi-active flapping propulsor is efficient over a wide range of operating conditions. This shows a possibility to practically use such self-pitching foil as a propulsion system.

## 1 INTRODUCTION

A fully-active flapping foil is the propulsion system where the foil heave and pitch kinematics are directly prescribed [1]. This system generally requires two actuators in order to drive both motions separately. Otherwise, a complex mechanism is required to simultaneously drive the two motions with one actuator. A numerical study based on inviscid model, i.e. Boundary Element Method (BEM), has shown that the fully-active flapping propulsor has high propulsive efficiency [2]. The prescribed pitch amplitude has been found to play a significant role in the range of operation bandwidth. For high pitch amplitude, the propulsor efficiently generates thrust for a relatively narrow range of equivalent advance numbers. A decrease in pitch amplitude tends to give a wider operation range.

In order to simplify the mechanical drive system, the use of spring-loaded oscillating foil, or in other name semi-active flapping propulsor, has been suggested [3, 4]. This system possesses only one actuator driving the foil heave motion while the foil pitch motion is passively adjusted

by interactions between hydrodynamic forces and a torsional spring attached to the foil hinge. Since this semi-active propulsor is a flow-induced vibration system, the spring stiffness as well as both foil and added inertias should influence the propulsive performance. In our previous study [5], the effects of inertia ratio and resonance on the open water characteristics of a semi-active flapping foil have been investigated using a BEM. The inviscid results show that the semi-active flapping propulsor performs efficiently over wide ranges of mechanical and kinematic conditions. The foil can efficiently generate thrust within the considered parametric range including the region where the instantaneous angle of attack is noticeably higher than the foil static stall angle [4].

Although the BEM has been mentioned as a useful approach to predict the unsteady forces generated by flapping foil [6], it should be pointed out that the BEM can sometimes lead to completely different results than the unsteady viscous solver. The disagreement between the both methods is due to a lack of boundary layer model in the potential flow approach. As a result, the inviscid solver may give an unreliable result at a certain range of operating conditions where serious flow separation occurs, e.g. high flapping frequency zone.

In an effort to investigate the effects of viscosity on the performance of fully-active flapping propulsor, different numerical tools have been used [7]. It has been reported that the BEM accurately predict hydrodynamic forces at high equivalent advance numbers due to its capability to model unsteady attached flows. However, in spite of similar trends in open water characteristics, simulations using a viscous solver result in lower efficiency than that of the potential flow code. As for the semi-active flapping propulsor, such viscous investigation has not been yet performed. In the present study, the inviscid results from our previous report concerning semi-active propulsor [5] will be compared to that of viscous approach.

## 2 SEMI-ACTIVE FLAPPING PROPULSOR

A semi-active flapping propulsor is a heaving foil attached to a torsional spring at its pivot point as schematically illustrated in Figure 1. The foil of span  $b$  and chord  $c$  is subjected to travel horizontally with a constant advance velocity  $U$  and to heave vertically with a sinusoidal motion at its hinge  $h(t) = h_0 \sin(2\pi ft)$ . The spring provides restoring moment toward static

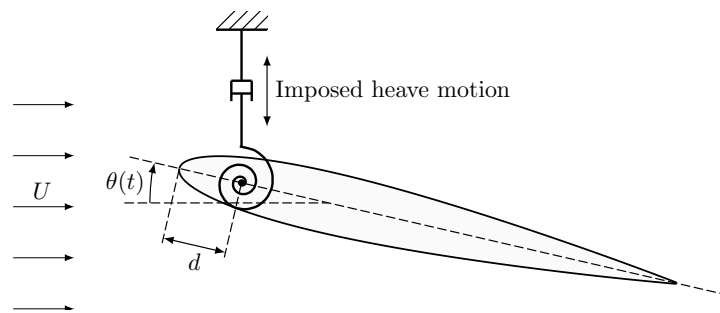


**Figure 1:** Schematic illustration of the semi-active flapping foil with imposed heave motion  $h(t) = h_0 \sin(2\pi ft)$ . The pitch angle  $\theta(t)$  is passively determined by hydrodynamic and spring forces.

equilibrium in which the foil lies horizontally and also parallelly to the advance velocity. The open water performance such as the propulsive efficiency  $\eta$  is characterized by dimensionless parameters:

$$\eta = \hat{\phi}(h^*, \Lambda, d^*, I^*, J_{\text{eq}}, r) \quad (1)$$

where  $h^* = h_0/c$  is the dimensionless heave amplitude,  $\Lambda = b/c$  is the wing aspect ratio,  $d^* = d/c$  is the dimensionless pivot location,  $I^* = I/I_w$  is the inertia ratio,  $I$  is foil moment of inertia, and  $I_w$  is moment of inertia of fluid volume displaced by the foil around the pitching axis. Note that the foil centre of mass is located at the pivot point.

The propulsive performance of flapping propulsor is traditionally presented as functions of reduced frequency  $k = \pi fc/U$  or alternatively Strouhal number  $St$ . However, in the present study, the open water characteristics of the foil is expressed in functions of advance ratio  $J = U/nD$  similarly to that of conventional marine propeller in order to be able to fairly compare both systems. This can be done by introducing an equivalent diameter for the flapping kinematics on the basis of similar swept area:  $D_{\text{eq}} = \sqrt{8h_0b/\pi}$ . The equivalent advance number can therefore be defined as  $J_{\text{eq}} = U/fD_{\text{eq}}$  which can be considered as another form of invert Strouhal number.

The last parameter in Eq. 1 is the frequency ratio representing the effects of spring stiffness and foil inertia:

$$r = \frac{f}{f_n} = 2\pi\sqrt{\frac{If^2}{K}} \quad (2)$$

where  $r$  is the structural frequency ratio,  $f_n$  is the natural frequency calculated based on the foil inertia  $I$ , and  $K$  is the torsional spring stiffness. It should be noted that the added inertia is not taken into account in the calculation of frequency ratio  $r$ . The effect of the added inertia has already been discussed in our previous study [5]. In order to investigate the influence of advance number as well as frequency ratio on the propulsive performance, the foil parameters are defined as shown in Table 1.

**Table 1:** Mechanical and kinematic parameters.

Dimensionless heave amplitude	$h^*$	2.0
Wing aspect ratio	$\Lambda$	5.0
Dimensionless pivot location	$d^*$	0.0
Inertia ratio	$I^*$	10.0
Equivalent advance number	$J_{\text{eq}}$	1.5 - 6.0
Frequency ratio	$r$	0.1 - 1.8

### 3 NUMERICAL TOOL

In the present study, the Lattice Boltzmann Method (LBM) approach provided by a commercial CFD solver XFlow 2018 of Dassault Systèmes is used to simulate the flow around the semi-active flapping propulsor. The implementation can be summarized as follow. This unsteady viscous solver uses distribution functions in order to describe the collective behaviour of several mesoscopic particles. The governing equation is the discrete Boltzmann equation:

$$f_i(x + c_i\delta t, t + \delta t) = f_i(x, t) + \Omega_i(x, t) \quad (3)$$

where  $f_i$  is the particle distribution function for discrete direction  $i$ ,  $c_i$  is the corresponding discrete velocity,  $\Omega_i$  is the collision operator. Macroscopic parameters of density and momentum are calculated using the equilibrium distribution function by:

$$\rho = \sum_{i=0}^{b-1} f_i \quad (4)$$

and

$$\rho u = \sum_{i=0}^{b-1} f_i c_i \quad (5)$$

respectively, where  $b$  is the number of discrete directions of particle velocities. The solver uses D3Q27 model with twenty seven velocities for three-dimensional flow.

Viscous effects are taken into account via a relaxation time parameter in the collision operator. In order to improve numerical stability and accuracy, a collision model based on multiple relaxation time (MRT) scheme is utilized [8]. This alternative meshless approach has characteristics of wall-adapting local eddy (WALE) which is applied for turbulence closure and near-wall treatment.

The flow around the semi-active flapping propulsor is simulated in a three-dimensional domain with the length, width and height of  $40c$ ,  $30c$  and  $30c$  respectively, where  $c$  is the chord length. The computational domain is considerably large so that the wall effect is negligible on the basis of a small blockage ratio. An adaptive refinement is applied in the vicinity of both foil and wake giving lattice node size of  $c/32$  as suggested by [7]. A time step size of  $dt = T/400$  is utilized in the LBM simulations which is considered sufficient to capture the flow physics. It has been found that the smaller time step provides the nearly coincident thrust production with the  $T/400$  case, whilst the larger time step gives a slight deviation.

## 4 RESULTS

The simulations have been performed for at least 5 flapping periods or until periodic solutions have been observed. The results presented in this section are obtained from the last 2 periods of simulations in which the solutions are periodic. The propulsive performance  $\eta$  of semi-active flapping propulsor are presented in the range of the equivalent advance number of  $1.5 \leq J_{eq} \leq 6.0$  and the frequency ratio of  $0.1 \leq r \leq 1.8$ .

### 4.1 Performance prediction

Contours of the simulated propulsive efficiency (—) along with lines of maximum angle of attack (- -) on the  $(J_{eq}, r)$  parametric space for different numerical tools are presented in Figure 2. The results show a similar trend in maximum angle of attack within the considered range of the parametric space. This consequently means that both inviscid and viscous solvers give nearly identical response in pitch motion. However, there is a deviation in the predicted propulsive efficiencies especially in high angle of attack regimes. For the LBM simulations, the extreme incidence angle together with the high frequency ratio leads to a drastic decrease in propulsive efficiency. In the zone of high frequency ratio and low advance number, a cycle-averaged drag can be observed for the LBM simulations, whereas thrust is still found for the BEM simulations.

Moreover, the LBM yields a slightly lower optimal efficiency ( $\eta \approx 82.0\%$ ) compared to that obtained by BEM ( $\eta \approx 87.4\%$ ). Nevertheless, the peaks approximately take place at the same location for both frequency ratio ( $r \approx 0.51$ ) and advance number ( $J_{eq} \approx 2.85$ ) as indicated by the markers  $\times$  in Figure 2(a) and 2(b).

In spite of the mentioned deviation in the performance predictions, the LBM results confirm that the semi-active flapping propulsor is efficient over a wide range of operating conditions.

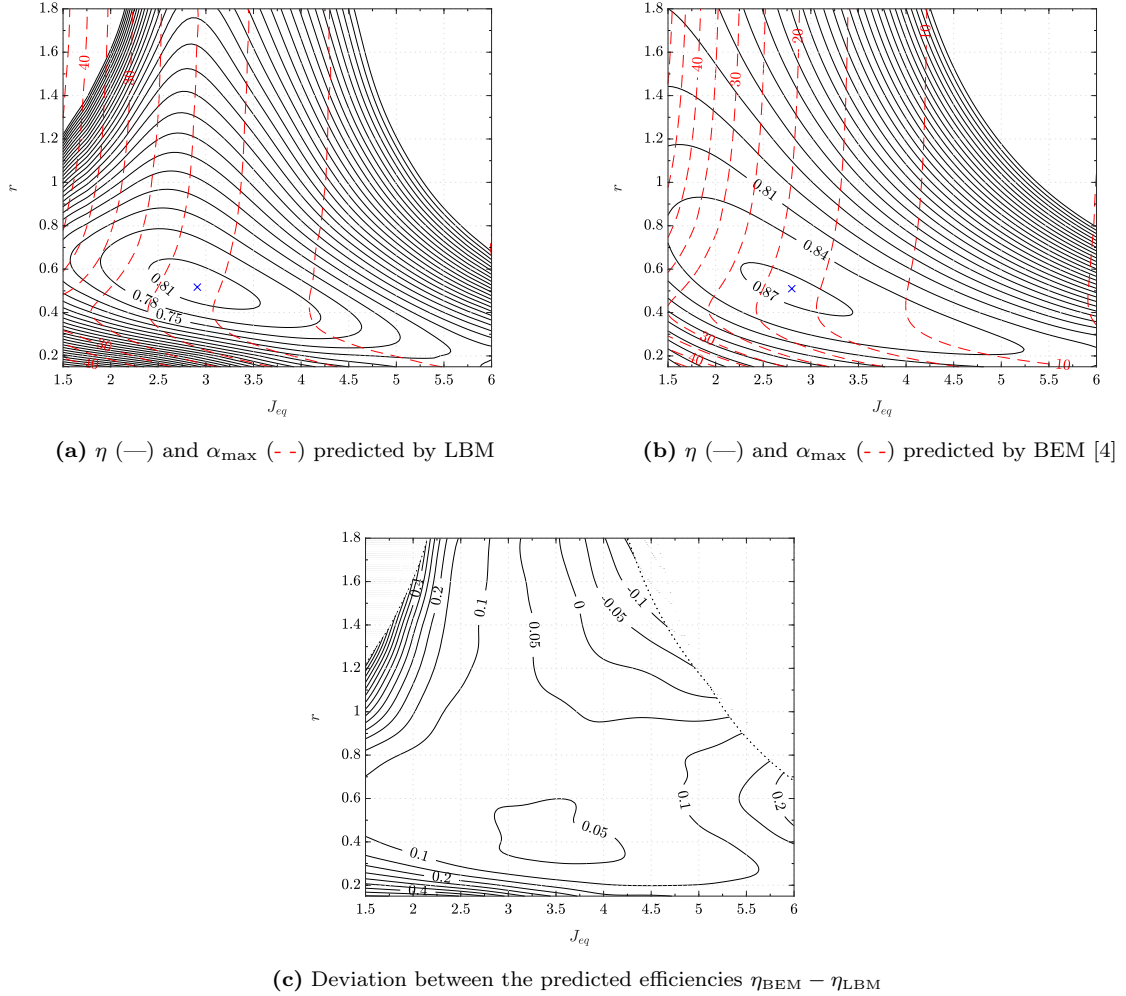


**Figure 2:** Performance of semi-active flapping foil as a function of equivalent advance number  $J_{eq}$  and frequency ratio  $r$ : (a) and (b) propulsive efficiency  $\eta$  along with the maximum angle of attack  $\alpha_{\max}$  predicted by LBM and BEM [4] respectively, (c) deviation of efficiency between BEM and LBM. The markers  $\times$  indicate the peak locations.

### 4.2 Deviation in efficiency prediction

When the propulsor operates at very low advance numbers, the kinematic conditions could momentarily give an angle of attack higher than the static stall angle, especially for very low and high frequency ratios, as shown in Figure 2(a) and 2(b). This is because the value of frequency ratio represents the spring stiffness as indicated by Eq. 2. The rigid spring (small frequency ratio) resists the foil from pitching, while the more elastic spring (high frequency ratio) leads to undesired pitching direction at the beginning of a new stroke. Both mechanisms together with high flapping frequency, i.e. small advance numbers, result in an effective angle of attack

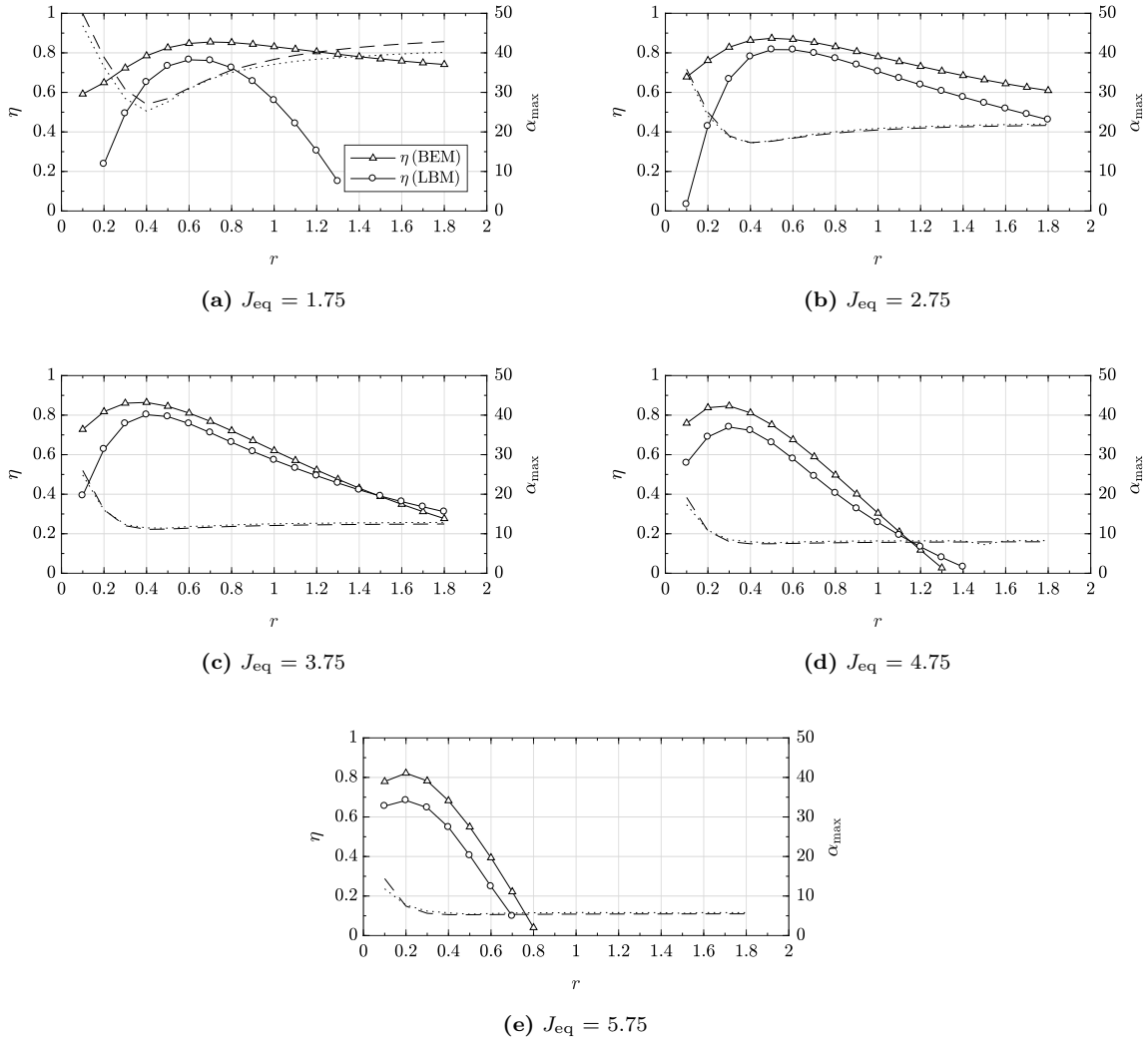


**Figure 3:** Propulsive efficiencies (solid lines with markers) as functions of frequency ratio for different equivalent advance numbers along with the maximum angle of attack  $\alpha_{\max}$  predicted by BEM (- -) and LBM ( $\cdots$ ) over a flapping period.

considerably greater than the foil static stall angle. In these extreme incidence angle cases, there is a noticeably deviation between the LBM and the BEM predictions (Figure 2(c)) as a result of flow separation.

The fully separation flow occurs and subsequently leads to a reduction in thrust and a rapid increase in required heave force. The force generation at this operating condition is therefore characterized by significant viscous effect which is not appropriately modeled using potential flow approach. Consequently, the deviation between BEM and LBM becomes obviously noticeable especially for both low and high frequency ratios, as seen in Figure 3(a). However, an appropriate range of frequency ratio ( $0.4 \leq r \leq 0.7$ ) could prevent the extreme incidence angle. The results of both numerical approaches become close to each other. Note that the efficiency in Figure 3 is calculated only in the case of thrusting mode.

For low to intermediate advance numbers, the instantaneous angle of attack becomes moderately higher than static stall angle, seemingly affect the reliability of the BEM results. However, it has been shown that the rapid change in angle of attack of the foil could delay the flow separation to higher incidences compared to its normal static stall case. The stall could be temporarily delayed to angle of attack approximately  $20^\circ$  to  $25^\circ$  depending on foil kinematics [9]. The thrust and propulsive efficiency predicted by LBM simulations are therefore enhanced by this delayed stall mechanism. On the other hand, the enhancement in the BEM case is a result of naturally attached flow of the potential approach. For these moderate advance numbers, e.g. Figure 3(b), the LBM results agree well with the BEM results despite different performance enhancement mechanisms. Nevertheless, the deviation becomes significant at small frequency ratio due to extreme angle of attack.

The angle of attack, when it is small or equivalent to the foil static stall angle, does not remarkably influence the predictive capability of the BEM. In case of large equivalent advance number, i.e. low flapping frequency and hence small angle of attack, the potential approach seemingly appears to simulate the semi-active propulsor with acceptable agreement despite a slight deviation between the open water characteristics as shown in Figure 3(c), 3(d) and 3(e). The deviation between the two approaches is likely due to viscous effects. However, the trend remains unchanged.

## 5 CONCLUSIONS

The open water characteristics of a semi-active flapping propulsor is numerically studied using LBM. The investigation shows satisfactory trend agreement between viscous and inviscid solvers when the angle of attack is small or moderate in spite of a slight deviation which seemingly results from viscous effects. In the cases where the angle of attack is considerably high, the BEM inaccurately predicts the hydrodynamic forces and performance of the semi-active propulsor due mainly to flow separation. The LBM results also confirm that the propulsive performance of such biomimetic foil is efficient over a wide range of operating conditions.

## ACKNOWLEDGEMENTS

The authors would like to acknowledge Phatcharak Buatee, Pongsit Payaptiva and Prawut Booranariththithawee for their contribution and generous supply of simulation results.

## REFERENCES

- [1] Thaweewat, N., Bos, F.M., van Oudheusden, B.W., Bijl, H. Numerical study of vortex-wake interactions and performance of a two-dimensional flapping foil. *In: 47th AIAA Aerospace Sciences Meeting, Orlando* (2009) **791**.
- [2] Floc'h, F., Phoemsapthawee, S., Laurens, J.M., Leroux, J.B. Porpoising foil as a propulsion system. *Ocean Engineering* (2012) **39**:53–61.
- [3] Bøckmann, E., Steen, S. Experiments with actively pitch-controlled and spring-loaded oscillating foils. *Applied Ocean Research* (2014) **48**:227–235.
- [4] Thaweewat, N., Phoemsapthawee, S. and Juntasaro, V. Semi-active flapping foil for marine propulsion. *Ocean Engineering* (2018) **147**:556–564.
- [5] Phoemsapthawee, S., Thaweewat, N. and Juntasaro, V. Influence of resonance on the performance of semi-active flapping propulsor. *Ship Technology Research* (2019) (Article in Press).
- [6] Mantia, M.L., Dabnichki, P. Effect of the wing shape on the thrust of flapping wing. *Applied Mathematical Modelling* (2011) **35**(10):4979–4990.
- [7] Posri, A., Phoemsapthawee, S., Thaweewat, N. Viscous investigation of a flapping foil propulsor. *IOP Conference Series: Materials Science and Engineering* (2018) **297** 012012.
- [8] Lallemand, P., Luo, L.S. Theory of the lattice Boltzmann method: Dispersion, dissipation, isotropy, Galilean invariance, and stability. *Physical Review E* (2000) **61**(6):6546.
- [9] Akbari, M.H., Price, S.J., Simulation of dynamic stall for a NACA 0012 airfoil using a vortex method. *Journal of Fluids and Structures* (2003) **17**(6):855–874.